We are IntechOpen, the world's leading publisher of Open Access books
Built by scientists, for scientists

4,800
Open access books available

122,000
International authors and editors

135M
Downloads

Our authors are among the

154
Countries delivered to

TOP 1%
most cited scientists

12.2%
Contributors from top 500 universities

CLARIVATE ANALYTICS
BOOK CITATION INDEX
INDEXED

WEB OF SCIENCE™

Selection of our books indexed in the Book Citation Index in Web of Science™ Core Collection (BKCI)

Interested in publishing with us?
Contact book.department@intechopen.com

Numbers displayed above are based on latest data collected.
For more information visit www.intechopen.com

Chapter

Building Envelope with Phase Change Materials

Liu Yang, Yan Liu, Yuhao Qiao, Jiang Liu and Mengyuan Wang

IntechOpen

Abstract

Based on recent investigations on building envelope with phase change materials from all over the world, we select the key scientific and technical issues including the thermal design methods, climatic and seasonal suitability and application, etc. The chapter mainly contains four parts: how to design building envelope with phase change materials, how to deal with issues on climatic and seasonal suitability of the technology, how to improve thermal performance of phase change materials applied in building envelope, and what is the application mode. The thermal design principle and a simple calculation method of building envelope with phase change materials are proposed by experiments. Thermal comfort pertaining to ASHRAE Standard 55 under different conditions is investigated, and an approach to estimate favorable climatic characteristics for building envelope with phase change materials is established. To exert the phase change materials applied in building envelope effectively, thermal transfer enhancement methods and application are also provided in the chapter. The chapter can be helpful for the development of building energy efficiency and the goal of zero and net zero energy.

Keywords: building envelope, phase change materials, thermal design, climatic and seasonal suitability, application

IntechOpen

1. Introduction

Building energy saving is essential to overall energy conservation from different sectors [1]. To build a comfortable indoor thermal environment, the energy consumption of air conditioning is increasing rapidly, which has negative impacts on sustainable development. Passive low-energy buildings are developed to solve the problem [2]. Improving thermal performance of building envelope is an effective approach to achieve a stable indoor thermal environment and reduce building energy consumption [3]. There are two main ways for the improvement of building envelope thermal performance. One is to reduce heat transfer coefficient (U-value) then decrease the heat flux of building envelope. Another is to increase thermal inertia of buildings to enhance the resistance to the changing of outdoor thermal environment [4, 5], especially in climate conditions with large daily temperature range, where remarkable energy efficiency performance could be achieved by improving building thermal stability [6, 7]. Adopting heavy structure (such as earth brick) is a traditional method for the improvement of building thermal stability [8]. However, the traditional approach is not suitable for achievement of satisfying

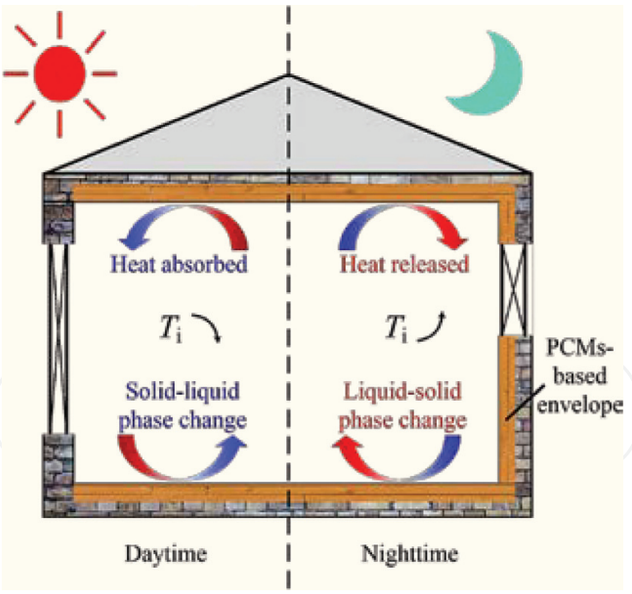

Figure 1.
Principle of PCM-based envelope.

thermal storage performance in lightweight structures widely developing in recent years. Due to large thermal capacity, phase change materials (PCMs) are ideal thermal storage materials to be integrated with building envelope [9]. As shown in **Figure 1**, building envelope integrated with PCMs can improve thermal inertia of lightweight structures and further stabilize indoor thermal environment [10]. Therefore, the thermal performance of PCM-based envelope has attracted more attention in recent years.

2. How to design building envelope with phase change materials

In this part, a kind of PCM-based lightweight wallboards which integrates PCMs with insulation materials is put forward. In application, the different PCM layer arrangements and the different PCM layout areas are significant to thermal performance of the wallboards. Current thermal design calculation of PCM-based envelope is mainly based on numerical methods. Although the numerical methods could obtain the wall temperature accurately, it is difficult to provide amounts of parameters and build models for architects. Therefore, in order to provide reference for the estimation of PCM-based envelope application effects, a thermal design calculation method is proposed, which is based on harmonic response method and equivalent specific heat capacity principle and is verified with experimental results. The present part mainly contains two points as follows: (1) a comparative experimental investigation with reduce-scale in the controlled condition, and (2) a simple thermal design method is developed based on harmonic response method and equivalent specific heat capacity principle.

2.1 Reduce-scale experiments

The experiments are conducted in the Thermal Storage and Ventilation Laboratory (TSVL) in Xi'an University of Architecture and Technology, Shaanxi, China. The lab consists of artificial climate chamber and control system, which can simulate the outdoor thermal environment including temperature and humidity. The temperature can be controlled by setting curves. Two test cells are adopted in the comparative experiments. The length, width, and height in each test cell are 1200mm, 660mm, and 800 mm, respectively. To exclude the uncontrollable factor

influence, the wallboards of test cell are made by 100 mm expandable polystyrene (EPS) panels which can be considered as adiabatic. In the experiments, PCM-based lightweight wallboard is adopted to replace one of EPS panel (see **Figure 2**). The macro-encapsulated PCM panels are employed in the experiments. The encapsulated PCMs are $CaCl_2 \cdot 6H_2O$, whose phase change temperature is 25–27°C. In melting process, the latent heat is 122.3 $kJ \cdot kg^{-1}$, and in solidification process the latent heat is 116.9 $kJ \cdot kg^{-1}$.

The experimental wallboard named PCM-based lightweight wallboard is put forward. The wallboard is made by 20 mm PCM layer and 30 mm insulation material layer. The wallboard improves its thermal storage capacity obviously by utilizing PCMs while sacrificing a fraction of insulation performance. The PCM-based lightweight wallboard is divided into PCM part and insulation part to distinguish whether there are PCMs in the horizontal direction.

r_A is defined as the ratio of PCM part area to wallboard area:

$$r_A = \frac{A_{PCM}}{A_{ALL}} \tag{1}$$

where A_{PCM} is the area of PCM and A_{ALL} is the area of the wallboard. The wallboards with four r_A are compared in experiments: 0, 21.6, 43.3, and 65%.

The reference group (r_A = 0%) is performed firstly to benchmark the PCM-based lightweight wallboard experiments. **Figure 3** shows the temperature curves of reference group during harmonic temperature changing process. Comparing the

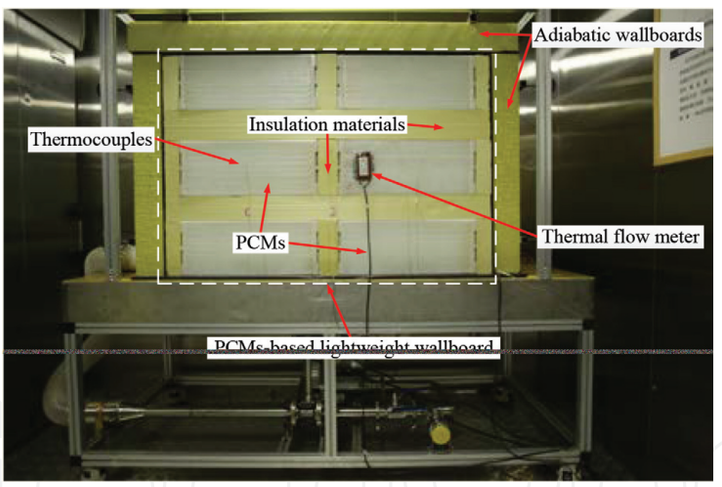

Figure 2.
PCM-based lightweight wallboard.

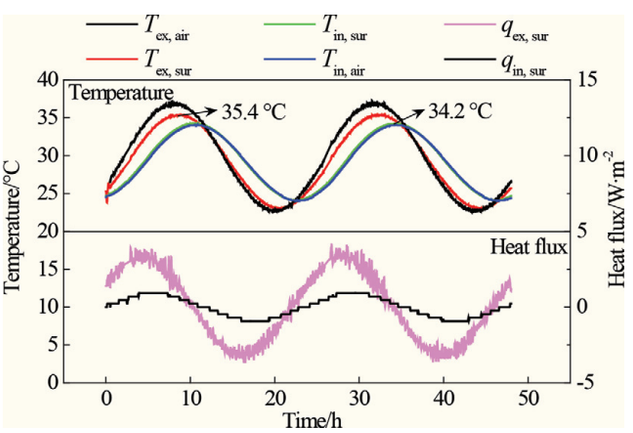

Figure 3.
Temperature under harmonic temperature fluctuation.

exterior and interior air temperature, the maximum temperature difference is 2.8° C, and the lag time is 2.5 h. The results prove that the insulation wallboard with poor thermal storage capacity is insufficient for the stability of indoor thermal environment.

Figure 4 shows the temperature and feat flux curves of the PCM-based lightweight wallboard (r_A = 65%) under harmonic temperature changing process. Due to the weak thermal inertia of insulation materials, the temperature changing of interior air is faster than the interior surface temperature changing of the PCM-based lightweight wallboard. It can be seen from the heat flux curves that the heat flux is delayed as much as 14.4 h. It is corresponding accurately between the largest temperature difference and the heat flux peak.

The temperature of the exterior/interior surfaces under the harmonic mode is shown in **Figure 5**. The temperature of interior surface and air is more stable in cell 1 (interior surface arrangement of PCM layer) than in cell 2 (exterior surface arrangement of PCM layer). The results show that the interior surface arrangement of PCM layer can reduce temperature amplitude in interior air to 32.1%. It proves that the PCM layer should be arranged on interior surface to improve thermal performance of PCM-based envelope.

Figure 6 illustrates the heat flux curves in PCM-based lightweight wallboards surfaces during the harmonic process. Because the PCMs are exposed to exterior air

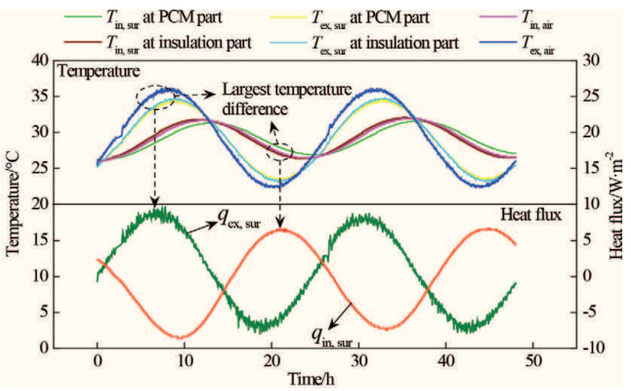

Figure 4.
Temperature and heat flux distribution of PCM-based lightweight wallboard during harmonic temperature process (r_A = 65%).

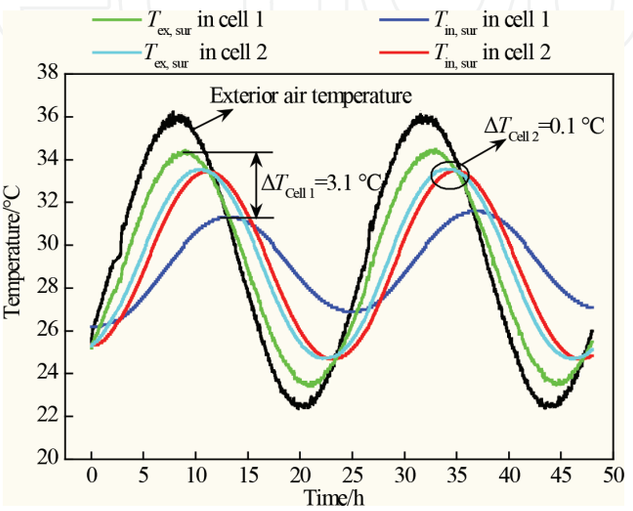

Figure 5.
Surface temperature curves during the harmonic process.

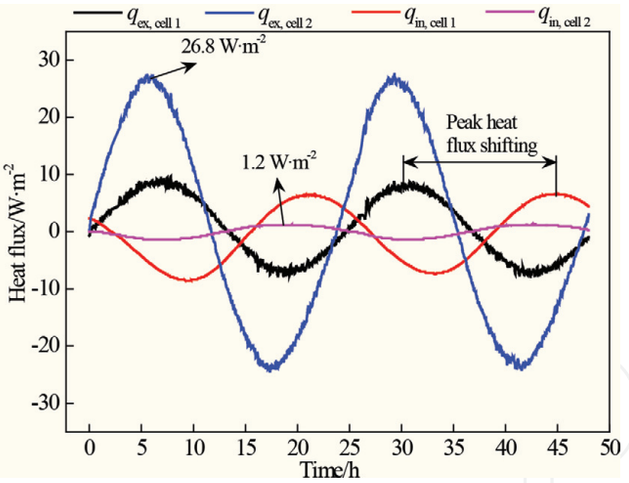

Figure 6.
Heat flux curves in PCM-based lightweight wallboards surfaces during the harmonic process.

in cell 2, the heat flux amplitude of exterior surface is larger than in cell 1. Meanwhile, because most of the incoming heat is absorbed by the PCM directly, the heat flux fluctuation on interior surface of cell 2 is less.

It can be proved by the experimental results that PCM layer with interior surface arrangement could achieve excellent performance to adjust indoor thermal environment. Although the PCM layer with exterior surface arrangement could absorb more heat from ambient environment, the PCMs cannot directly regulate the indoor thermal environment. By absorbing indoor excess heat, the PCM layer on interior surface can stabilize the indoor thermal environment. Therefore, it is a suitable approach to arrange the PCM layer on the interior surface of building envelope in the thermal design.

2.2 Thermal design method

As a traditional thermal design method of building envelope, harmonic response method can obtain the temperature fluctuation attenuation and delay time of normal envelope such as concrete and brick structures [11]. The method is widely accepted by engineers [12]. A simple thermal design method named HR-EC (harmonic response method and equivalent specific heat capacity principle) is proposed based on harmonic response method and equivalent specific heat capacity principle. The PCM-based envelope is different from normal envelope. During the phase change process, the latent heat will cause changing apparent specific heat. Therefore, to conveniently calculate the impact of latent heat, the calculation method adopts the equivalent specific heat capacity principle to simplify latent heat [13]. The temperature amplitude and delay time of interior surface of PCM-based lightweight wallboard are calculated and verified by comparing with the experimental results.

The HR-EC thermal design method is based on the harmonic response method, which is developed based on heat transfer analysis through building walls using Fourier transforms. Harmonic response method is a simple calculation method to obtain temperature damping and time delay of the walls without the analysis of heat transfer process. Therefore, it is a useful approach in the PCMs envelope thermal design.

Damping factor (v_0) of outdoor air temperature to wall interior surface temperature can be calculated as [12]

$$v_0 = 0.9e^{\frac{\Sigma D}{\sqrt{2}}} \cdot \frac{S_1 + \alpha_i}{S_1 + Y_{1,e}} \cdot \frac{S_2 + Y_{1,e}}{S_2 + Y_{2,e}} \cdot \ldots \frac{S_n + Y_{n-1,e}}{S_n + Y_{n,e}} \cdot \frac{\alpha_e + Y_{n,e}}{\alpha_e} \tag{2}$$

where ΣD is thermal inertia of building wall, S_n is coefficient of heat accumulation of wall materials, $Y_{n,e}$ is coefficient of heat accumulation of the outer surface of material layer, α_i is interior surface coefficient of heat transfer, and α_e is exterior surface coefficient of heat transfer.

D is thermal inertia of wall material layer. It can be defined as

$$D = R \cdot S \tag{3}$$

where R is thermal resistance of wall material layer and S is coefficient of heat accumulation of wall material. Thermal inertia represents the performance of material layers to resist the effects of fluctuating temperature, which is reflected by the temperature fluctuations of back of the material layer. ΣD can be obtained as

$$\Sigma D = D_1 + D_2 + \cdots + D_n \tag{4}$$

where D_1, $D_2 \ldots D_n$ are the thermal inertia of each material layer of the wall.

S_n and Y_n are expressed as follows [12]:

$$S_n = \sqrt{\frac{2\pi\lambda c\rho}{Z}} \tag{5}$$

$$Y_n = \frac{R_n S_{n^2} + Y_{n-1}}{1 + R_n Y_{n-1}} \tag{6}$$

where λ is thermal conductivity, c is specific heat capacity, ρ is wall materials density, and Z is period of temperature fluctuation.

Phase delay (Φ_0) between the maximum temperature of outdoor air and the maximum temperature of wall interior surface is calculated by [12]

$$\Phi_0 = 40.5\sum D + \arctan\frac{Y_{ef}}{Y_{ef} + \alpha_e\sqrt{2}} - \arctan\frac{\alpha_i}{\alpha_i + Y_{if}\sqrt{2}} \tag{7}$$

where Y_{ef} is coefficient of heat accumulation of wall outer surface and Y_{if} is coefficient of heat accumulation of wall inner surface. Because the temperature period is 24 h in building thermal design, the delay time (ξ_0) can be obtained as [12]

$$\xi_0 = \frac{Z}{360}\Phi_0 = \frac{1}{15}\Phi_0 \tag{8}$$

Building envelope is always affected by double-side thermal effects including indoor and outdoor temperature changes. Therefore, the damping factor (v_{if}) and time delay (Φ_{if}) between indoor air and interior surface temperature of building envelope should also be obtained by the following Equations [12]:

$$v_{if} = 0.95\frac{\alpha_i + Y_{if}}{\alpha_i} \tag{9}$$

$$\Phi_{if} = \arctan\frac{Y_{if}}{Y_{if} + \alpha_i\sqrt{2}} \tag{10}$$

$$\xi_{\mathrm{if}} = \frac{Z}{360}\Phi_{\mathrm{if}} = \frac{1}{15}\Phi_{\mathrm{if}} \tag{11}$$

It is necessary to determine the calculation parameters. The equivalent specific heat capacity principle is adopted to convert the latent heat to a constant value. The equivalent specific heat capacity (c_{p}) is defined as [13].

$$c\mathrm{p} = \begin{cases} c_{\mathrm{p}}^{\mathrm{L}} & (T > T\mathrm{L}) \\ c_{\mathrm{p}}^{\mathrm{M}} + c_{\mathrm{p}}^{*} & (T\mathrm{L} \geq T \geq T\mathrm{S}) \\ c_{\mathrm{p}}^{\mathrm{S}} & (T\mathrm{S} > T) \end{cases} \tag{12}$$

where $c_{\mathrm{p}}^{\mathrm{L}}$ is the specific heat capacity in liquid phase, $c_{\mathrm{p}}^{\mathrm{S}}$ is the specific heat capacity in solid phase, and $c_{\mathrm{p}}^{\mathrm{M}}$ is the average value of $c_{\mathrm{p}}^{\mathrm{L}}$ and $c_{\mathrm{p}}^{\mathrm{S}}$; c_{p}^{*} can be calculated as [13]

$$c_{\mathrm{p}}^{*} = \frac{\Delta h}{\Delta T_{\mathrm{R}}} \tag{13}$$

where ΔT_{R} is the temperature range during the complete phase change process and Δh is the latent heat of phase change process. Δh is obtained as

$$\Delta h = \Delta H \cdot ratio \tag{14}$$

where ΔH is the latent heat of the PCM and *ratio* is the phase change ratio of PCMs during phase change process. In the phase change process, the thermal conductivity of the PCM is also replaced as equivalent thermal conductivity [13]:

$$\lambda_{\mathrm{p}} = \begin{cases} \lambda_{\mathrm{p}}^{\mathrm{L}} & (T > T\mathrm{L}) \\ \lambda_{\mathrm{p}}^{\mathrm{S}} + \dfrac{\lambda_{\mathrm{p}}^{\mathrm{L}} - \lambda_{\mathrm{p}}^{\mathrm{S}}}{\Delta T_{\mathrm{R}}} & (T\mathrm{L} \geq T \geq T\mathrm{S}) \\ \lambda_{\mathrm{p}}^{\mathrm{S}} & (T\mathrm{S} > T) \end{cases} \tag{15}$$

where $\lambda_{\mathrm{p}}^{\mathrm{S}}$ is the thermal conductivity in solid phase and $\lambda_{\mathrm{p}}^{\mathrm{L}}$ is the thermal conductivity in liquid phase.

The results are listed in **Table 1**. The calculated results are close to the experimental results with 7.7% relative error. The results of interior surface temperature delay time have larger relative error with 33.2%. As an estimated method used in early design, the method is an easy way to predict the trend of temperature amplitude and delay time.

For the calculation of temperature damping factor and delay time by HR-EC method, the input parameters of wall materials are necessary to be determined, including thermal conductivity (λ), density (ρ), specific heat capacity (c), and material layer thickness (d). In addition, the equivalent specific heat capacity (c_{p}) is also a significant parameter for the calculation of PCM-based envelope thermal

	Calculated results	Experimental results	Relative error (%)
Temperature amplitude	4.06°C	4.40°C	7.7
Temperature delay time	3.38 h	5.06 h	33.2

Table 1.
Calculated and experimental results of PCM-based lightweight wallboard.

performance. It is critical to determine the phase change ratio in phase change process. In this part, it is determined based on experimental results. To provide references for PCM-based envelope thermal design in buildings, the phase change ratio of PCM-based envelope in different climate conditions could be obtained by series of further experiments.

3. How to deal with issues on climatic and seasonal suitability of the technology

The purpose of the present work is to investigate the seasonal and climatic suitability for application of PCM-based envelope coupled with night ventilation (NV) strategy in naturally ventilated office buildings. For suitability analysis, the adaptive thermal comfort theory is applied and the adaptive comfort model in standard ASHRAE-55 is adopted [14].

3.1 Numerical simulation details

Dynamic thermal simulations are performed using EnergyPlus. All simulations are carried out from April 1 to October 31, which covers the whole cooling season. The weather data is accessed based on the standard CSWD weather files provided by EnergyPlus [15]. The Conduction Finite Difference (CondFD) solution algorithm is adopted to depict the thermal process of phase change layer. The Fully Implicit Order is selected as the difference scheme for CondFD [16]. According to the suggestion of Tabares-Valesco et al. [17], time step for CondFD in EnergyPlus is set to 3 min, and node space is set to 3. The other components of the envelope are modeled with the default Conduction Transfer Functions algorithm. The heat conduction between the ground and the floor is calculated by Ground Heat Transfer: Slab module. TARP and DOE-2 are adopted for the interior and exterior surface convective heat transfer algorithms, respectively [18]. To perform NV strategy, the Zone Ventilation: Wind and Stack Open Area module is employed [19].

Three-dimensional model and standard floor plan of the office building are depicted in **Figure 7**. The four-storey building is 3.6 m storey height, 31.9 m length, and 15.8m width. The total floor area is 2016 m^2. The size of each window is 1.8m height and 1.5 m width. The window-wall ratio is 16.3% of the north and south walls and 5.1% of the remaining walls, which satisfies local standard [20].

According to Ref. [21], it has been verified that phase change temperature (*PCT*) has great influence on thermal performance of PCMs in different seasons.

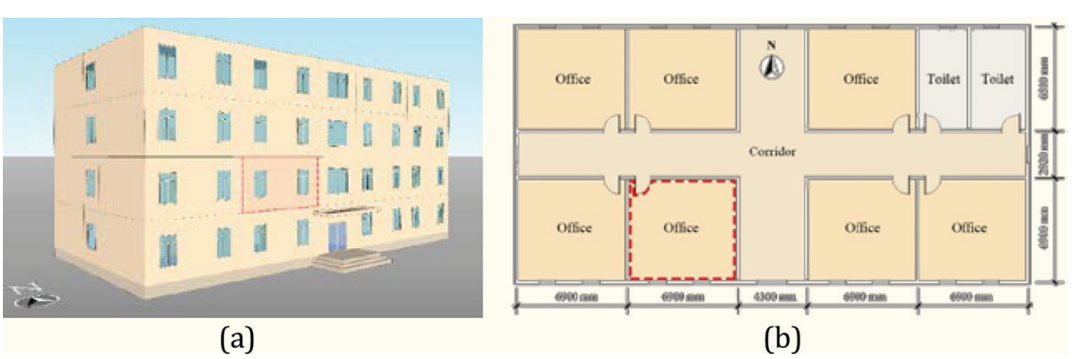

Figure 7.
(a) The 3D model and (b) the standard floor plan of the building for EnergyPlus simulation.

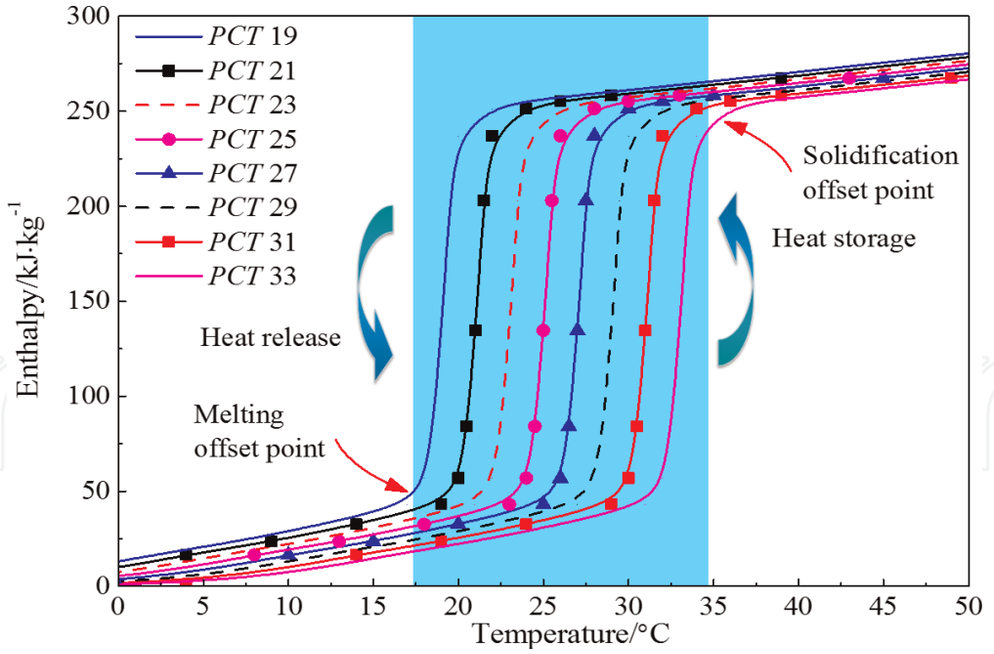

Figure 8.
H-T curves of eight different PCMs.

Therefore, to examine the climatic and seasonal suitability of *PCT*, Bio-PCMs with eight different *PCT* are adopted. The enthalpy-temperature graph of Bio-PCMs is depicted in **Figure 8** [22]. The latent heat of Bio-PCMs is 219 $kJ \cdot kg^{-1}$. The density is 860 $kg \cdot m^{-3}$ and the specific heat is 1.97 ($kJ \cdot kg^{-1} \cdot {}^{o}C^{-1}$). The thermal conductivity is 0.2 ($W \cdot m^{-1} \cdot {}^{o}C^{-1}$). Bio-PCMs are installed on the inner side of building envelope (external walls, internal walls and ceilings) in Ref. [23].

3.2 Evaluation index

With the adaptive comfort theory, Evola et al. [24] proposed an index called Intensity of Thermal Discomfort (*ITD*), to evaluate the indoor thermal environment. It is defined as the time integral, over the occupancy period of the positive difference between the current operative temperature and the upper limit of thermal comfort range (see **Figure 9**). This index reveals well the duration and the extent of discomfort thermal sensation perceived by the occupants within a long period. Therefore, it is employed to represent the thermal performance of PCMs coupled with NV strategy. The calculation is expressed as follows:

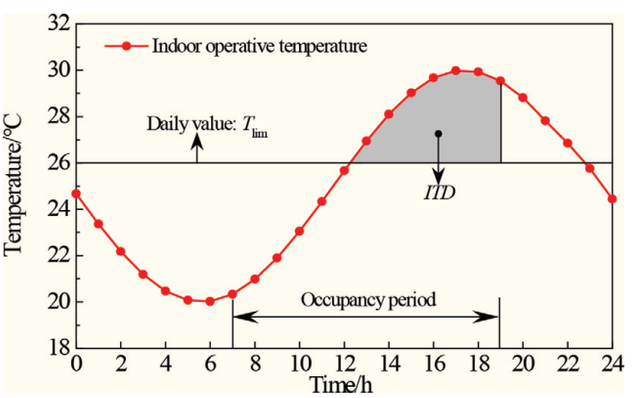

Figure 9.
Definition of ITD.

$$ITD = \int_{P} \Delta T^{+}(\tau) \cdot d\tau$$
$$\text{where } \Delta T^{+}(\tau) = \begin{cases} T_{op}(\tau) - T_{lim} & \text{if } T_{op}(\tau) \geq T_{lim} \\ 0 & \text{if } T_{op}(\tau) < T_{lim} \end{cases} \quad (16)$$

$$T_{lim} = 0.31 \cdot T_{rm} + 21.3 \quad (17)$$

where T_{op} is the operative temperature, T_{lim} is the upper threshold of 80% acceptability limit of Adaptive Comfort Model in Standard ASHRAE-55 [14], and T_{rm} is the mean monthly outdoor air dry-bulb temperature, which is the arithmetic average of the mean daily minimum and mean daily maximum outdoor air dry-bulb temperature for the month in sequence.

3.3 Climatic and seasonal suitability analysis

A series of parametric studies over the selected eight Bio-PCMs are carried out, to investigate the suitability of *PCT* in transition and hot seasons. The optimum *PCT* for transition season and hot season is determined according to the minimum *ITD*, which are listed in **Table 2**. It can be found that in some cities, the optimal *PCT* for transition season does not match with the climate conditions in hot season, vice versa. Therefore, it is quite necessary to select different *PCT* based on the outdoor climatic characteristics of transition and hot seasons, respectively.

Based on the optimum *PCT*, the effect of PCMs coupled with NV strategy on reducing *ITD* in transition and hot seasons is compared with NV strategy and PCMs strategy. **Figure 10** summarizes the *ITD* in both transition and hot seasons with different technologies in all cities. All strategies (with PCMs coupled with NV strategy, with NV strategy, and with PCMs strategy) can reduce *ITD* compared with reference group (without cooling strategy). The *ITD* of transition season is shown in **Figure 10(a)**. For these cities in hot summer and warm winter zone, the effects with PCMs alone in reducing *ITD* are inferior to NV strategy. It is evident for Nanning and Hechi, where the *ITD* with PCMs is much higher than that with NV. When NV is introduced on the basis of PCMs strategy, *ITD* is reduced from 2231 to

Cities	Optimum *PCT*/°C	
	Transition season	Hot season
Turpan	27	33
Nanning	29	29
Hechi	27	29
Chongqing	27	29
Xi'an	25	27
Chengdu	25	27
Urumqi	23	25
Altay	23	25
Guiyang	23	25
Kunming	23	23

Table 2.
Optimum PCT for transition season and hot season.

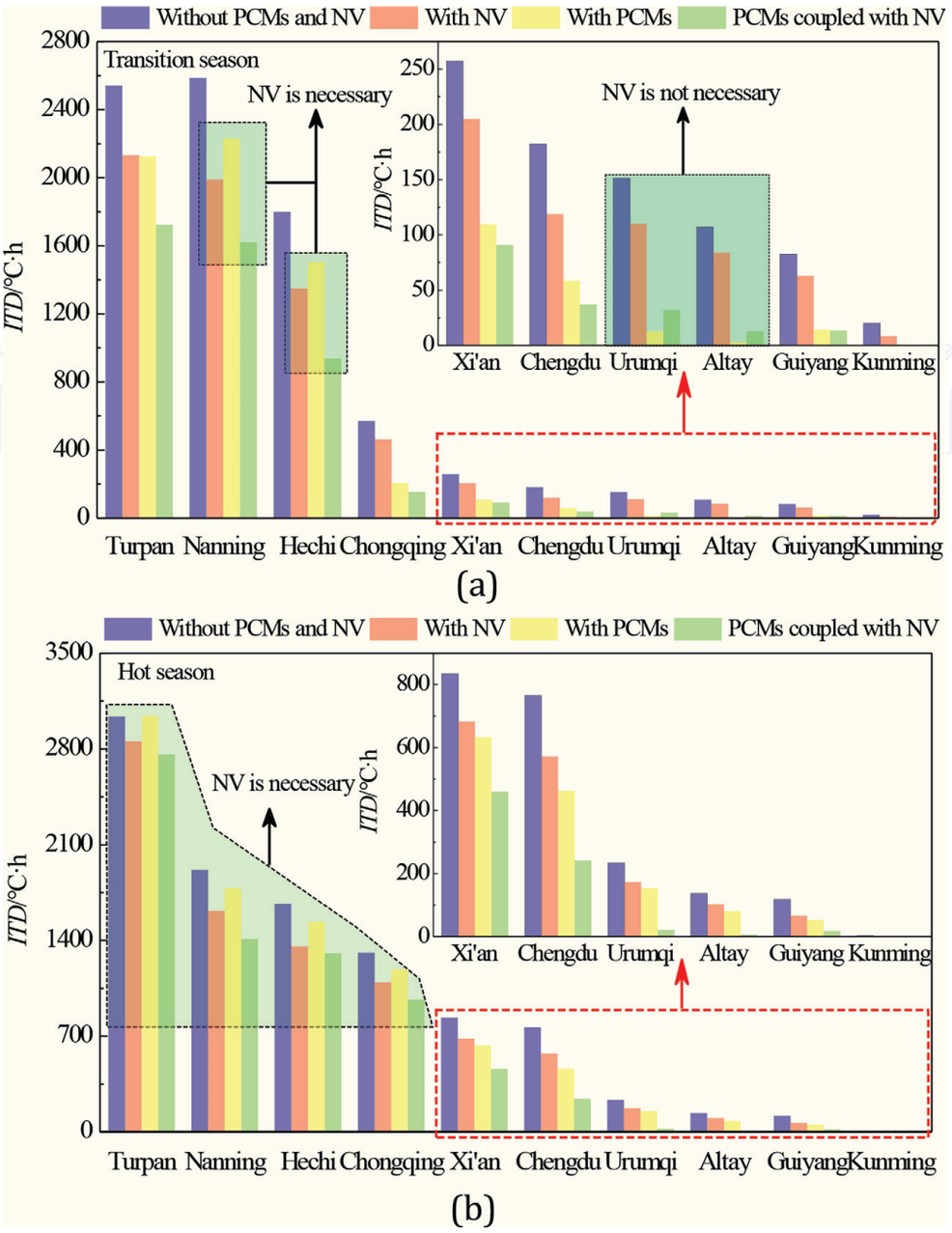

Figure 10.
(a) Transition season and (b) hot season of the influence of different passive cooling technologies on ITD.

1621°C·h for Nanning and from 1503 to 937°C·h for Hechi. It is due to NV strategy working well to introduce outdoor cool air into the room and to exclude the heat released from PCMs to outdoor during nighttime. Accordingly, PCMs can be fully solidified at night. Therefore, *ITD* can be effectively decreased during the occupancy period using PCMs coupled with NV. It further indicates the coupling use of NV strategy, and PCMs strategy is necessary for transition season under this climate condition. On the contrary, PCMs coupled with NV strategy is inferior to PCMs strategy for severe cold zones. It is clear that *ITD* is increased when PCMs coupled with NV strategy is adopted in Urumqi and Altay compared to PCM strategy. Such results indicate that PCM strategy is more suitable to severe cold zone in transition season rather than PCMs coupled with NV strategy. For other cities, PCMs coupled with NV strategy is more suitable in transition season in reducing *ITD* compared to NV strategy and PCM strategy.

From **Figure 10(b)**, PCMs coupled with NV is the most effective strategy to reduce *ITD* in hot season for all cities. However, the advantages of PCMs coupled

with NV strategy than NV strategy in Turpan, Nanning, Hechi, and Chongqing are greatly reduced compared to transition season due to the high temperature and small diurnal temperature difference in hot season. Additionally, with PCM strategy alone, *ITD* in these cities is much higher than that with NV strategy or PCMs coupled with NV strategy. It indicates that NV strategy is necessary for PCM strategy to obtain excellent performance. The use of PCMs coupled with NV strategy is critical to hot season.

A performance-based inverse design method is proposed to extract typical outdoor air dry-bulb temperature from typical meteorological year, which is favorable for application of PCMs coupled with NV. The typical air dry-bulb temperature curve (T_{out}) is obtained as **Figure 11** shown (Nanning, China). Outdoor air dry-bulb temperature fluctuation range is much larger than the phase transition temperature range (27–31°C). Meanwhile, the maximum value T_{max} (33°C) is 2°C higher than the upper limit of *PCT*, and the minimum value T_{min} (25.5°C) is 1.5°C lower than the lower limit of *PCT*. In other words, PCMs could have an opportunity to solidify at low temperature phase and to melt at high temperature phase. Additionally, the average value T_{ave} (28.6°C) is quite close to *PCT* 29°C, and the diurnal temperature difference (ΔT) is greater than 7.5°C. These conditions are beneficial to the utilization of latent heat of PCMs.

Figure 12 is the comparison of T_{out} and outdoor air dry-bulb temperature in a typical week (1–7 June). T_{out} agrees well with outdoor air dry-bulb temperature curve. It means the approach can be used to determine T_{out} curve.

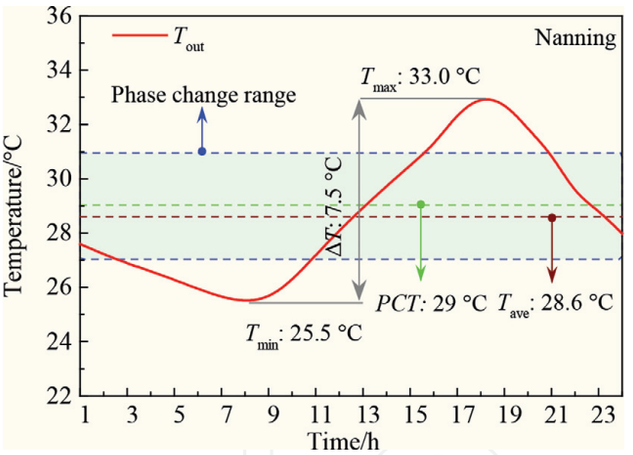

Figure 11.
Characteristics of the typical outdoor air dry-bulb temperature curve.

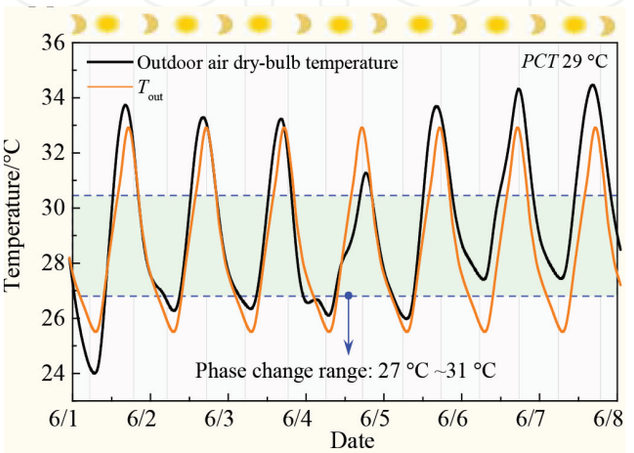

Figure 12.
Comparison between T_{out} and outdoor air dry-bulb temperature in a typical week.

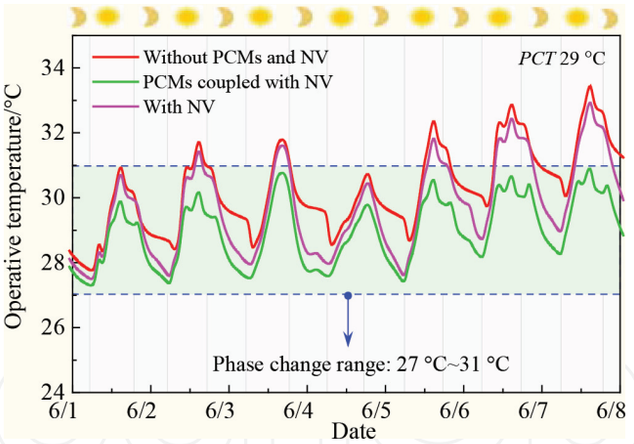

Figure 13.
Indoor operative temperature in the typical week: PCMs coupled with NV vs. NV.

In order to verify the reliability of the method, indoor operative temperature using PCMs coupled with NV and NV in the typical week is compared in **Figure 13**. PCMs coupled with NV appear as a remarkable advantage in reducing indoor operative temperature than NV. Indoor operative temperature reduction is up to 1°C, even to 2°C in 6–8 June. It can infer that outdoor air dry-bulb temperature in the typical week is beneficial to PCMs coupled with NV. It further indicates that the method is reliable. Therefore, it can be used to estimate the relationship between PCMs coupled with NV strategy and local outdoor climatic characteristics.

4. How to improve thermal performance of phase change materials applied in building envelope

Taking PCMs into building envelope significantly reduces building energy consumption and improves indoor thermal environment. The main categories of PCMs applied in building envelope are organic PCMs and inorganic PCMs. They both have solid–liquid phase flow properties, and the phase transition takes place at a certain temperature range. Paraffin is the most commonly used organic because it has chemically stable, high latent of fusion, and regular degradation in thermal properties after phase change cycles. However, paraffin has low thermal conductivity, flammable, and slow oxidation when exposed to oxygen. These problems present challenges in container design [25]. Salt hydrates as an important group of inorganic PCMs have extensively investigated in building envelope. The most serious limitation of the salt hydrates is phase segregation and supercooling compared with paraffin. Another problem is salt hydrates would cause corrosion in building materials and metal containers. These problems limit their applications in building envelope [26].

The integration of PCMs and building envelope can be divided into three types: direct incorporation and immersion, macro-encapsulation, and micro-encapsulation (see **Figure 14**). Using PCMs in building envelope, one must keep in mind that liquid phase causes leaking to the surface out of the carrier materials. Encapsulation serves as barrier between PCM and surrounding environment. It provides long-term durability and structural requirements. Micro-encapsulation of PCMs provides faster charging and discharging rates because of the smaller distance for heat transfer compared to macro-encapsulation. However, the lower encapsulation rate of micro-encapsulation greatly reduced the energy storage and increases the cost [27].

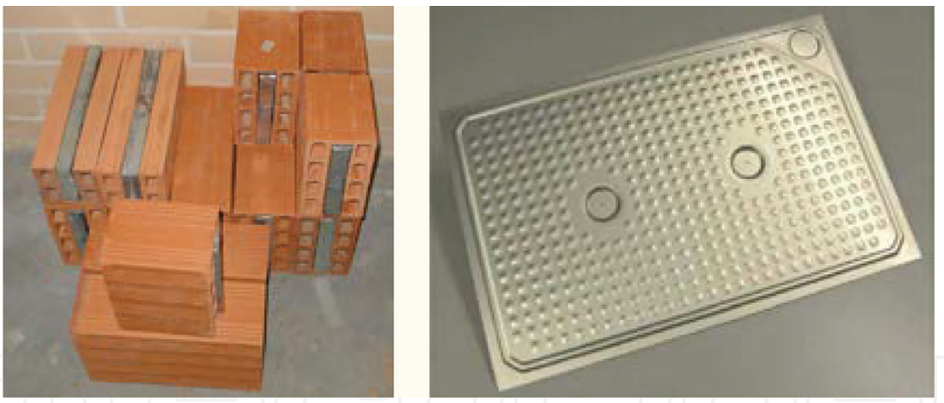

Figure 14.
Macro-encapsulation of PCMs applied in building envelope [28, 29].

4.1 Heat transfer enhancement at material level

Among the different combinations of PCMs and building envelope, macro-encapsulation (building component with PCMs) is considered as a promising option in building energy conservation. The advantages of the technique embodied at various packaging shapes and sizes includes avoiding leakage of material, providing sufficient thermal storage capacity, and reducing the adverse effects on structure, whereas unreasonable application and poor thermal conductivity would cause the regulating ability of indoor thermal environment untimely and incompletely. The building applications require fast absorption and release of latent heat. In addition, small temperature fluctuation is not beneficial to the utilization of PCMs in buildings. Hence, heat transfer enhancement of PCMs is significant for building envelope. The heat transfer performance of PCMs building component can enhance at material level and component level [30]. At material level, carbon-based materials are one of the most common additives due to high thermal conductivity, stable chemical performance, and low density. However, uniformly dispersion of additives in PCMs is the most important factor to improve thermal conductivity. Moreover, aspect ratio of additives is also crucial for thermal conductivity enhancement such as carbon fiber (CF) and carbon nanotubes (CNTs).

At material level, CNTs is selected as a heat transfer medium for the composite PCM in experiment. A group of the composite PCM is prepared with CNTs of 0.5, 1, 1.5, and 2 wt%. The thermal conductivity and latent heat are determined and compared. The experimental results show that thermal conductivity of the composite PCM with 2 wt% CNTs increased by 17 and 21% compared to pure paraffin in liquid and solid phase, respectively.

To evaluate the heat storage and release capacity of pure paraffin and the composite PCM, the infrared thermograph images of two samples are recorded in **Tables 3** and **4**. It can be found that the heat transfer rate of the composite PCM is greatly improved both in heat release and heat storage process. Especially, the average temperature of the composite PCM at different time is 2°C higher than that of pure paraffin in heat storage process. Moreover, the temperature distribution of the composite PCM is more uniform than that of pure paraffin in heat storage process.

4.2 Heat transfer enhancement at component level

At component level, metal fins are widely used to increase the heat transfer areas and relatively easy to fabricate for building component with PCMs [31]. The main

Time		0 min	10 min	20 min	30 min	Legend
Heat release	Pure paraffin	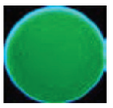				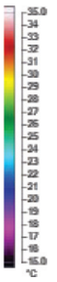
	T_{ave}	26°C	24.7°C	23.2°C	23.1 °C	
	Composite PCM					
	T_{ave}	26°C	24.1°C	23.0°C	22.8 °C	

Table 3.
Heat release comparison of pure paraffin and the composite PCM.

Time		0 min	5 min	10 min	15 min	Legend
Heat storage	Pure paraffin		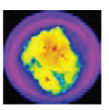	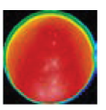	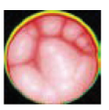	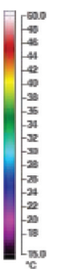
	T_{ave}	22.5°C	36.9°C	45.2°C	48.3°C	
	Composite PCM		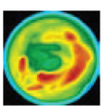			
	T_{ave}	22.2°C	38.8°C	47.6°C	49.3°C	

Table 4.
Heat storage comparison of pure paraffin and the composite PCM.

Time	45 min	60 min	75 min	90 min	Legend
Non-optimized component (top and bottom)	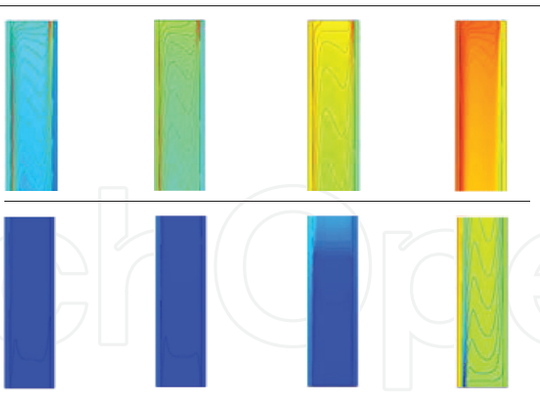				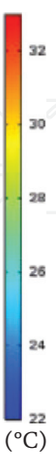
Optimized component (top and bottom)	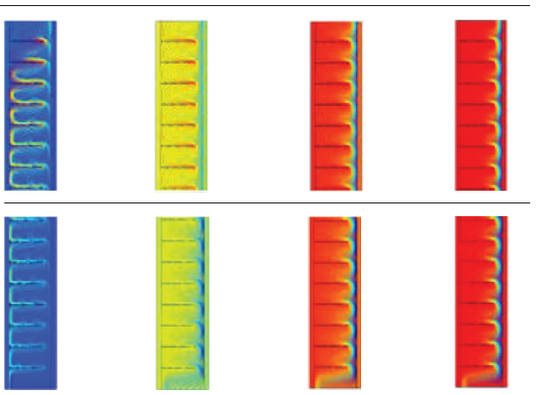				(°C)

Table 5.
Comparisons of optimized/nonoptimized component with PCMs.

influence factors on thermal performance of PCMs component are fins number and geometry. The current research works mainly focused on the effect of fins number or geometry separately. However, these two factors should be taken into consideration. To enhance heat transfer rate, the balance between fins number and geometry should be further investigated.

In the field of PCMs heat transfer, numerical method is widely employed by architects. To obtain the appropriate geometric of fins, the building component with PCMs is optimized by COMSOL Multiphysics. The results show that PCMs complete melting time in the building component and the temperature difference of heat transfer surfaces could be used to evaluate the fins effect. The optimized building component presents the best heat transfer performance with 8 mm length, 0.2 mm width, and 5 mm spacing of fins. The temperature comparison of building component with PCMs before and after optimization is shown in **Table 5**. It can be seen that the heat transfer performance of the optimized component is better than non-optimized component during heat storage process. The temperature difference between top and bottom in the non-optimized component is increasing over the time. It directly gives the fact that appropriate geometry of fins makes the heat transfer much more uniform and reduce the adverse effect of natural convection in heat storage process.

5. What is the application mode?

PCMs coupled with NV are an effective passive cooling strategy for office buildings. A kind of inorganic PCMs encapsulated in PVC panel developed by a Chinese manufacturer is applied in building envelope as a wall application in a naturally ventilated office building. According to differential scanning calorimeter (DSC) test [32], the latent heat of the PCM is 122.3 $kJ \cdot kg^{-1}$ in melting and 116.9 $kJ \cdot kg^{-1}$ in solidification. The phase change temperature range is 25–27°C. The thickness of PVC panel is 20 mm, and the length and width are 520 mm and 200 mm. The PCM panel is installed at the interior surface of an external wall and an internal wall of the office building through modular installation as shown in **Figure 15**. The PCM panel is directly connected to the wall using aluminum strips and nuts by the modular installation.

For north wall, the PCM panel is directly installed on the interior surface (see **Figure 16(a)**). The PCM panel exposed to indoor air is beneficial to convection heat transfer between indoor air and the PCM panel. At nighttime, the outdoor cool air is introduced into indoor space through the opened window. When the cold air flows through the PCM-based wall, the coldness is stored by PCMs. For south wall, the

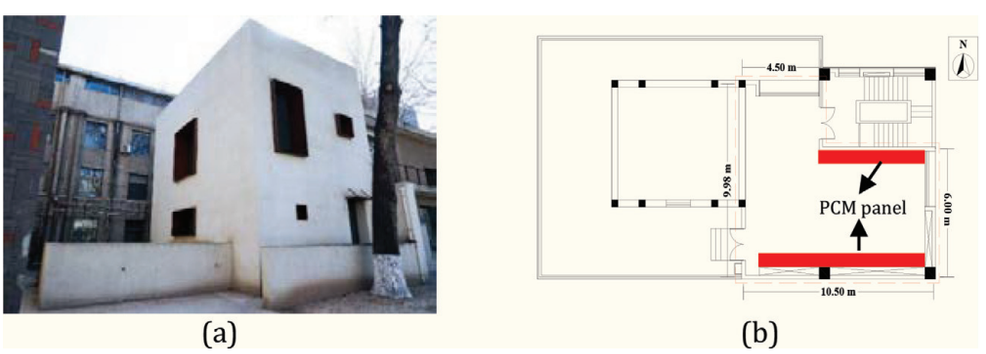

Figure 15.
(a) Isometric view of the naturally ventilated office building and (b) diagram of installation position of PCM panel.

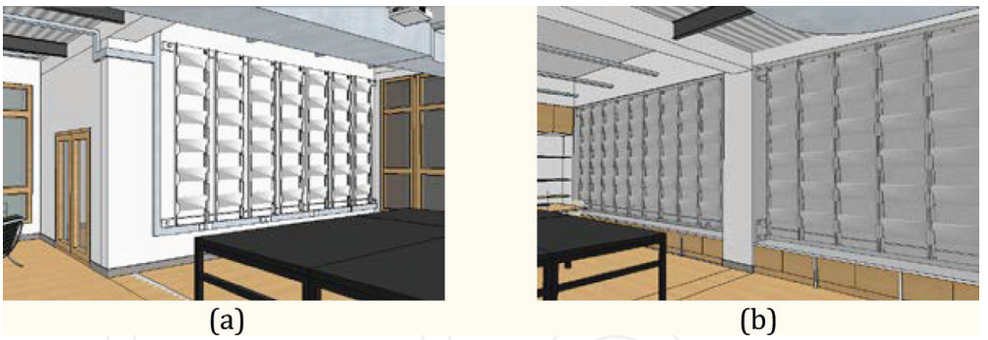

Figure 16.
(a) Design sketch, PCM panel exposed to indoor air; and (b) design sketch, PCM panel decorated with perforated aluminum plate.

installation of the PCM panel is the same as that of the north wall. However, considering that there is a constructional column in the middle of the south wall protruding into the interior space, the exterior of the PCM panel is decorated with perforated aluminum plate. These tiny holes in the aluminum plate can promote the convection heat transfer between indoor air and the PCM panel (see **Figure 16(b)**).

Actual installation effect of the PCM panel is shown in **Figure 17**. To examine the application effect of PCMs coupled with NV strategy in hot season, full-scale field thermal environment test is conducted in a typical week of hot season. Indoor air temperature, surface temperature, and heat flux of the wall with the PCM panel are carefully investigated. To obtain the cooling potential of PCMs coupled with NV, the scenario of the wall without the PCM panel is modeled using EnergyPlus with the actual weather data during the test period. The accuracy and reliability of the method is validated by comparing the simulated and experimental results with maximum relative error of 2.95% and average relative error of 0.96%.

The indoor thermal environment before and after the application of PCMs coupled with NV is compared with experiment and simulation results. It can be observed from **Figure 18(a)** that the interior surface heat flux of the wall with the PCM panel is significantly greater than that without the PCM panel. It demonstrates that PCMs absorb and release a lot of heat from indoor air during the melting or solidification process. Therefore, the interior surface peak temperature of the wall with the PCM panel is greatly reduced with respect to wall without the PCM panel as shown in **Figure 18(b)**. Accordingly, the indoor air peak temperature is greatly reduced using the PCM panel. The maximum reduction of indoor air temperature is up to 1.1°C (see **Figure 18(c)**).

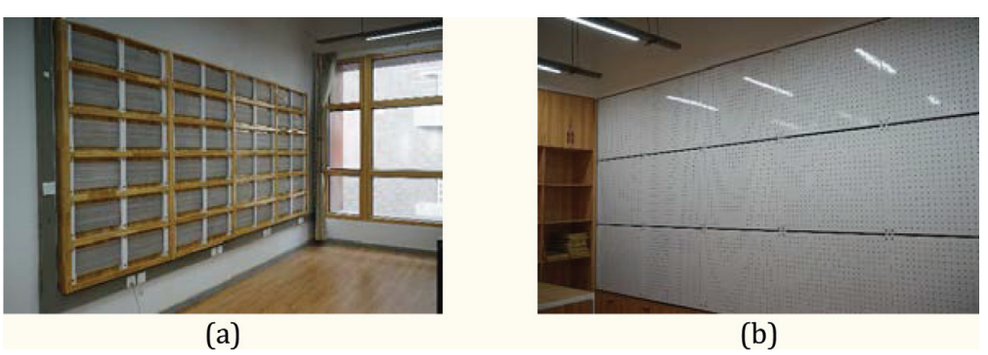

Figure 17.
Actual installation effect of the PCM panel: (a) exposed to indoor air and (b) decorated with perforated aluminum plate.

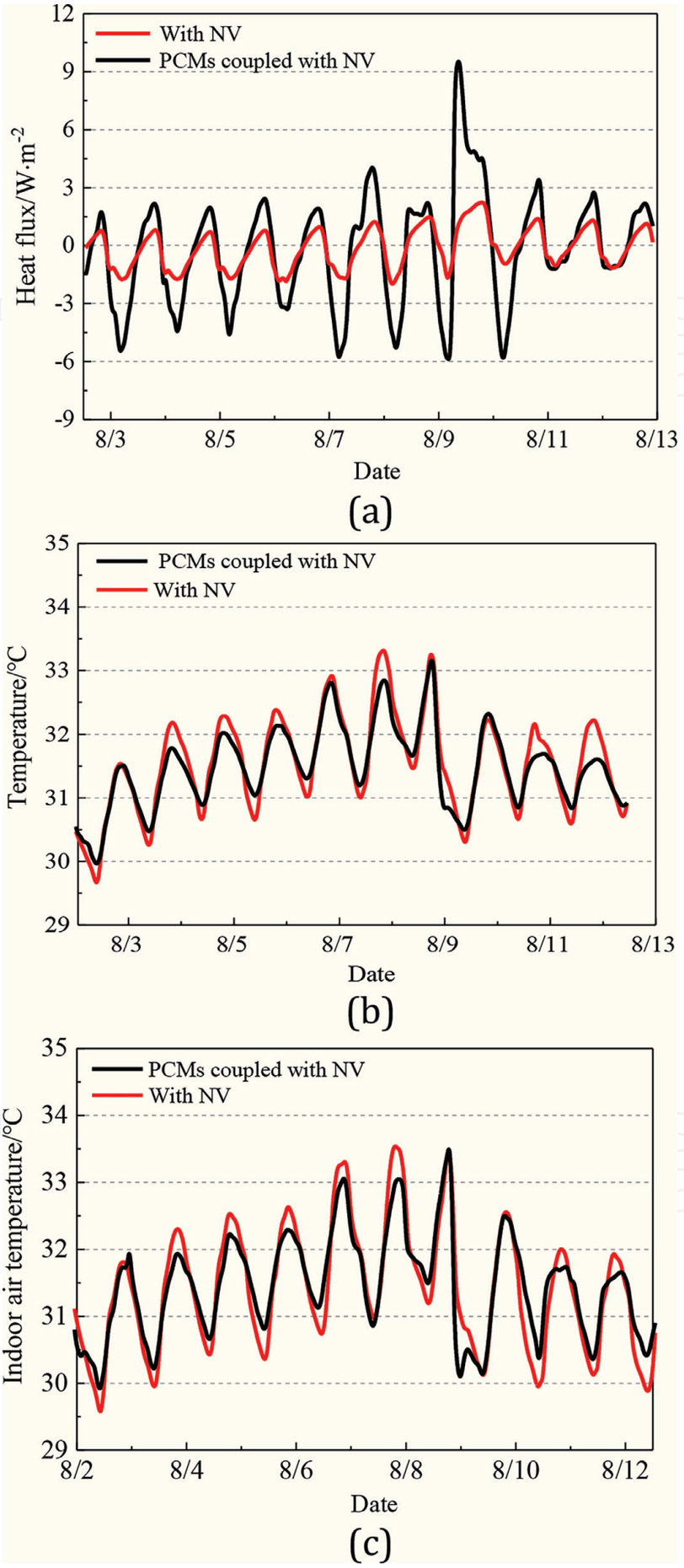

Figure 18.
(a) Interior surface heat flux of north wall, (b) interior surface temperature of north wall, and (c) indoor air temperature.

6. Conclusions

1. Comparative experimental investigations of thermal performance of PCM-based lightweight wallboards are conducted in the artificial controlled condition with harmonic temperature changing. The thermal performance of PCM-based lightweight wallboards is carefully analyzed. Two kinds of controlled conditions are compared: different PCM layout areas and different PCM layer arrangements are adopted. Moreover, a simple thermal design method is proposed and verified with the artificial controlled experimental results.

2. A typical naturally ventilated office building has been modeled with EnergyPlus, and several simulations have been carried out based on 10 representative cities of Western China. The climatic and seasonal suitability for application of PCMs coupled with NV strategy is investigated from three aspects: suitability of *PCT*, comparisons of three different cooling strategies, and application advantage. Moreover, a performance-based inverse design method is proposed to determine the typical climate characteristics.

3. Based on two methods of thermal transfer enhancement of PCMs applied in building envelope, PCMs and building component with PCMs are optimized in material and component level, respectively. The optimum proportion of CNTs in the composite PCM is obtained through experiment. Appropriate geometry of fins is optimized by numerical simulation. Results show that two optimization methods can promote the heat transfer performance of PCMs and improve the utilization of PCMs.

4. A kind of PCM panel is applied as wall application in a naturally ventilated office building. Full-scale field indoor thermal environment test is conducted in a typical week of hot season. The thermal performance of the wall with PCM panel is superior to the wall without the PCM panel. The heat storage capacity of the wall can be improved by 40%, and the indoor air peak temperature can be reduced by 1.1°C in the test period of hot season.

Acknowledgements

This work was supported by “the 13th Five-Year” National Science and Technology Major Project of China (No. 2018YFC0704500), Natural Science Foundation of China (No. 51838011 and No. 51808429), Shaanxi Province Key Research and Development Plan (No. 2017ZDXM-SF-076), China Postdoctoral Science Foundation (No. 2018 T111026), and Natural Science Foundation of Shaanxi Province (No. 2017JQ5005).

Conflict of interest

We declare that there is no conflict of interest exits in the chapter, as well as the chapter is approved by all authors for publication.

Nomenclature

A_{ALL}	Area of the wallboard, m^2
A_{PCM}	Area of PCM, m^2

c	Specific heat capacity of materials, $kJ \cdot kg^{-1} \cdot {}^{o}C^{-1}$
c_p	Equivalent specific heat capacity, $kJ \cdot kg^{-1} \cdot {}^{o}C^{-1}$
D	Thermal inertia of wall material layer, dimensionless
d	Thickness of wall materials, m
ITD	Intensity of thermal discomfort, °C·h
PCT	Phase change temperature, °C
$q_{ex,sur}$	Heat flux of exterior surface, $W \cdot m^{-2}$
$q_{in,sur}$	Heat flux of interior surface, $W \cdot m^{-2}$
R	Thermal resistance of wall material layer, $m^2 \cdot {}^{o}C \cdot W^{-1}$
r_A	Ratio of PCM part area to wallboard area, dimensionless
$ratio$	Phase change ratio of PCMs during phase change process, %
S	Coefficient of heat accumulation of wall materials, $W \cdot m^{-2} \cdot {}^{o}C^{-1}$
T_{ave}	Average value of typical outdoor air dry-bulb temperature, °C
$T_{ex.air}$	Exterior air temperature, °C
$T_{ex.sur}$	Temperature of the exterior surface, °C
$T_{in,air}$	Interior air temperature, °C
$T_{in.sur}$	Temperature of the interior surface, °C
T_{lim}	Upper threshold of 80% acceptability limit of Adaptive Comfort Model in Standard ASHRAE-55, °C
T_{max}	Maximum value of typical outdoor air dry-bulb temperature, °C
T_{min}	Minimum value of typical outdoor air dry-bulb temperature, °C
T_{op}	Operative temperature, °C
T_{out}	Typical outdoor air dry-bulb temperature, °C
T_{rm}	Mean monthly outdoor air dry-bulb temperature, °C
v_{if}	Damping factor between indoor air and interior surface temperature of building envelope, dimensionless
v_0	Damping factor of outdoor air temperature to wall interior surface temperature, dimensionless
Y_{ef}	Coefficient of heat accumulation of wall outer surface, $W \cdot m^{-2} \cdot {}^{o}C^{-1}$
Y_{if}	Coefficient of heat accumulation of wall inner surface, $W \cdot m^{-2} \cdot {}^{o}C^{-1}$
$Y_{n,e}$	Coefficient of heat accumulation of the outer surface of material layer, $W \cdot m^{-2} \cdot {}^{o}C^{-1}$
Z	Period of temperature fluctuation, h

Greek letters

α_e	Exterior surface coefficient of heat transfer, $W \cdot m^{-2} \cdot {}^{o}C^{-1}$
α_i	Interior surface coefficient of heat transfer, $W \cdot m^{-2} \cdot {}^{o}C^{-1}$
ΔH	Latent heat of the PCM, $kJ \cdot kg^{-1}$
Δh	Latent heat of phase change process, $kJ \cdot kg^{-1}$
ΔT	Diurnal temperature difference, °C
ΔT_R	Temperature range during the complete phase change process, °C
ΔT^+	Difference between operative temperature and comfort temperature, °C
λ	Thermal conductivity of materials, $W \cdot m^{-1} \cdot {}^{o}C^{-1}$
λ_p	Thermal conductivity of PCMs, $W \cdot m^{-1} \cdot {}^{o}C^{-1}$
ξ_{if}	Delay time between the highest indoor temperature and the inner surface temperature of wall, h
ξ_0	Delay time between the highest outdoor temperature and the inner surface temperature of wall, h
ρ	Density of materials, $kg \cdot m^{-3}$
Φ_{if}	Phase difference between the highest indoor temperature and the inner surface temperature of wall, deg

Φ_0	Phase difference between the highest outdoor temperature and the inner surface temperature of wall, deg

Abbreviations

CF	Carbon fiber
CondFD	Conduction finite difference
CNTs	Carbon nanotubes
DSC	Differential scanning calorimeter
EPS	Expandable polystyrene
HR-EC	Harmonic response method and equivalent specific heat capacity principle
NV	Night ventilation
PCMs	Phase change materials
TSV	Thermal storage and ventilation
TSVL	Thermal storage and ventilation laboratory

Author details

Liu Yang[1,2*], Yan Liu[1,2], Yuhao Qiao[1,2], Jiang Liu[1,2] and Mengyuan Wang[1,2]

1 State Key Laboratory of Green Building in Western China, Xi'an University of Architecture and Technology, Xi'an, Shaanxi, P.R. China

2 School of Architecture, Xi'an University of Architecture and Technology, Xi'an, Shaanxi, P.R. China

*Address all correspondence to: yangliu@xauat.edu.cn

IntechOpen

© 2019 The Author(s). Licensee IntechOpen. This chapter is distributed under the terms of the Creative Commons Attribution License (http://creativecommons.org/licenses/by/3.0), which permits unrestricted use, distribution, and reproduction in any medium, provided the original work is properly cited. CC BY

References

[1] Souayfane F, Fardoun F, Biwole PH. Phase change materials (PCM) for cooling applications in buildings: A review. Energy and Buildings. 2016;**129**: 396-431. DOI: 10.1016/j.enbuild.2016.04.006

[2] Liu Y, Yang L, Zheng WX, Liu T, Zhang XR, Liu JP. A novel building energy efficiency evaluation index: Establishment of calculation model and application. Energy Conversion and Management. 2018;**166**:522-533. DOI: 10.1016/j.enconman.2018.03.090

[3] Yang L, Lam JC, Tsang CL. Energy performance of building envelopes in different climate zones in China. Applied Energy. 2008;**85**(9):800-817. DOI: 10.1016/j.apenergy.2007.11.002

[4] Navarro L, Gracia AD, Niall D, Castell A, Browne M, Mccormack SJ. Thermal energy storage in building integrated thermal systems: A review. Part 2. Integration as passive system. Renewable Energy. 2016;**85**(2): 1334-1356. DOI: 10.1016/j.renene.2015.06.064

[5] Liu Y, Yang L, Hou LQ, Li SY, Yang J, Wang QW. A porous building approach for modelling flow and heat transfer around and inside an isolated building on night ventilation and thermal mass. Energy. 2017;**141**: 1914-1927. DOI: 10.1016/j.energy.2017.11.137

[6] Lam JC, Yang L, Liu JP. Development of passive design zones in China using bioclimatic approach. Energy Conversion and Management. 2006; **47**(6):746-762. DOI: 10.1016/j.enconman.2005.05.025

[7] Liu J, Liu Y, Yang L, Hou LQ, Wang MY, Liu JP. Annual energy saving potential for integrated application of phase change envelopes and HVAC in Western China. Procedia Engineering. 2017;**205**:2470-2477. DOI: 10.1016/j.proeng.2017.09.975

[8] Li DHW, Yang L, Lam JC. Zero energy buildings and sustainable development implications—A review. Energy. 2013;**54**(6):1-10. DOI: 10.1016/j.energy.2013.01.070

[9] Zhang YP, Lin KP, Zhang Q, Di HF. Ideal thermophysical properties for freecooling (or heating) buildings with constant thermal physical property material. Energy and Buildings. 2006; **38**(10):1164-1170. DOI: 10.1016/j.enbuild.2006.01.008

[10] Kuznik F, David D, Johannes K, Roux JJ. A review on phase change materials integrated in building walls. Renewable and Sustainable Energy Reviews. 2011;**15**(1):379-391. DOI: 10.1016/j.rser.2010.08.019

[11] Zhou JL, Zhang GQ, Lin YL, Li YG. Coupling of thermal mass and natural ventilation in buildings. Energy and Buildings. 2008;**40**(6):979-986. DOI: 10.1016/j.enbuild.2007.08.001

[12] Chinese National Standard. Thermal Design Code for Civil Building (GB 50176–1993). Beijing: Ministry of Housing and Urban-Rural Development of the People Republic of China; 1993. [in Chinese]

[13] Chou HM, Chen CR, Nguyen VL. A new design of metal-sheet cool roof using PCM. Energy and Buildings. 2013; **57**(1):42-50. DOI: 10.1016/j.enbuild.2012.10.030

[14] ASHRAE Standard 55-2010. Thermal Environmental Conditions for Human Occupancy. Atlanta: American Society of Heating, Refrigerating and Air-conditioning Engineers; 2010

[15] EnergyPlus: Weather Data [Internet]. 2019. Available from: https://

www.energyplus.net/weather [Access Time: 06-10-2019]

[16] Al-Saadi SN, Zhai ZQ. Modeling phase change materials embedded in building enclosure: A review. Renewable and Sustainable Energy Reviews. 2013;**21**:659-673. DOI: 10.1016/j.rser.2013.01.024

[17] Tabares-Velasco PC, Christensen C, Bianchi M. Verification and validation of EnergyPlus phase change material model for opaque wall assemblies. Building and Environment. 2012;**54**: 186-196. DOI: 10.1016/j.buildenv.2012.02.019

[18] EnergyPlus: Engineering Reference [Internet]. 2019. Available from: https://www.energyplus.net/documentation [Access Time: 06-01-2019]

[19] Jamil H, Alam M, Sanjayan J, Wilson J. Investigation of PCM as retrofitting option to enhance occupant thermal comfort in a modern residential building. Energy and Buildings. 2016; **133**:217-229. DOI: 10.1016/j.enbuild.2016.09.064

[20] Chinese National Standard. Design Standard for Energy Efficiency of Public Buildings (GB 50189-2015). Beijing: Ministry of Housing and Urban-Rural Development of the People Republic of China; 2015. [in Chinese]

[21] Saffari M, Gracia AD, Fernández C, Cabeza LF. Simulation-based optimization of PCM melting temperature to improve the energy performance in buildings. Applied Energy. 2017;**202**:420-434. DOI: 10.1016/j.apenergy.2017.05.107

[22] Muruganantham K. Application of phase change material in buildings: Field data vs EnergyPlus simulation [thesis]. Arizona: Arizona State University; 2010

[23] Cui YP, Xie JC, Liu JP, Wang JP, Chen SQ. A review on phase change material application in building. Advances in Mechanical Engineering. 2017;**9**(6):1-15. DOI: 168781401770082

[24] Evola G, Marletta L, Sicurella F. A methodology for investigating the effectiveness of PCM wallboards for summer thermal comfort in buildings. Building and Environment. 2013;**59**: 517-527. DOI: 10.1016/j.buildenv.2012.09.021

[25] Sharma SD, Sagara K. Latent heat storage materials and systems: A review. International Journal of Green Energy. 2005;**2**(1):1-56. DOI: 10.1081/GE-200051299

[26] Baetens R, Jelle BP, Gustavsen A. Phase change materials for building applications: A state-of-the-art review. Energy and Buildings. 2010;**42**(9): 1361-1368. DOI: 10.1016/j.enbuild.2010.03.026

[27] Akeiber H, Nejat P, Majid MZA, Wahida MA, Jomehzadeh F, Famileh IZ, et al. A review on phase change material (PCM) for sustainable passive cooling in building envelopes. Renewable and Sustainable Energy Reviews. 2016;**60**: 1470-1497. DOI: 10.1016/j.rser.2016.03.036

[28] Silva T, Vicente R, Soares N, Ferreira V. Experimental testing and numerical modelling of masonry wall solution with PCM incorporation: A passive construction solution. Energy and Buildings. 2012;**49**:235-245. DOI: 10.1016/j.enbuild.2012.02.010

[29] Castell A, Martorell I, Medrano M, Pérez G, Cabeza LF. Experimental study of using PCM in brick constructive solutions for passive cooling. Energy and Buildings. 2010;**42**(4):534-540. DOI: 10.1016/j.enbuild.2009.10.022

[30] Liu LK, Su D, Tang YJ, Fang GY. Thermal conductivity enhancement of phase change materials for thermal energy storage: A review. Renewable

and Sustainable Energy Reviews. 2011; **15**(1):24-46. DOI: 10.1016/j.rser.2010.08.007

[31] Ma T, Yang HX, Zhang YP, Lu L, Wang X. Using phase change materials in photovoltaic systems for thermal regulation and electrical efficiency improvement: A review and outlook. Renewable and Sustainable Energy Reviews. 2015;**43**:1273-1284. DOI: 10.1016/j.rser.2014.12.003

[32] Yang L, Qiao YH, Liu Y, Zhang XR, Zhang C, Liu JP. A kind of PCMs-based lightweight wallboards: Artificial controlled condition experiments and thermal design method investigation. Building and Environment. 2018;**144**: 194-207. DOI: 10.1016/j.buildenv.2018.08.020

IntechOpen